ISSN 0031-918X, The Physics of Metals and Metallography, 2007, Vol. 104, No. 1, pp. 13–18. © Pleiades Publishing, Ltd., 2007.
Original Russian Text © S.S. Aplesnin, N.I. Piskunova, 2007, published in Fizika Metallov i Metallovedenie, 2007, Vol. 104, No. 1, pp. 17–21.

THEORY OF METALS

Formation of Magnetic Order in $Ca_{1-x}R_xMnO_3$ (R = La, Pr, Sm)

S. S. Aplesnin[a, b] and N. I. Piskunova[a]

[a] *Siberian State Aerospace University, pr. im. gazety "Krasnoyarskii rabochii" 31, Krasnoyarsk, 660014 Russia*
[b] *Kirenskii Institute of Physics, Siberian Division, Russian Academy of Sciences, Akademgorodok, Krasnoyarsk, 660036 Russia*

Received December, 1, 2006

Abstract—The regions of existence of magnetic structures of the G and C type and the region of their coexistence have been found in $Ca_{1-x}R_xMnO_3$ (R = La, Pr, Sm) solid solutions using the Monte Carlo method. A phase diagram on the temperature–concentration plane has been calculated in the model with random and ordered distribution of anisotropic ferromagnetic bonds.

PACS numbers: 61.50.Ah, 75.47.Lx

DOI: 10.1134/S0031918X07070034

1. INTRODUCTION

The oxides of transition metals of the $R_{1-x}A_xMnO_3$ type (R = La, Pr, Nd, Sm, etc.; A = Ca, Sr, Ba, Pb) are in the last years an object of extensive experimental and theoretical investigations. The properties of these manganites change substantially depending on the concentration of the divalent ion; a number of phase transitions are observed with various types of structural, magnetic, charge, and orbital ordering. The most attractive properties of these compounds are electrical conductivity and effect of giant magnetic resistance (GMR). The main physical and theoretical properties of manganites have been considered in a number of reviews (see, e.g., [1–3]). The main attention in various investigations has been paid to the range of concentrations of $x < 0.5$ in view of the existence of the effect of colossal magnetoresistance in this range at high temperatures, which makes these compounds attractive for the application in spintronics.

The magnetic-field effect on transport properties is also observed at large concentrations ($x \approx 0.9$), but at lower temperatures ($T < 120$ K) [4]. At these concentrations, the type of order changes from the G to C type and charge ordering is developed, which is accompanied by distortions of crystal structure. The main problem is to establish the mechanism of the effect of giant magnetic resistance. One of factors responsible for this effect can be changes in the magnetic structure caused by charge ordering.

A spatially nonuniform distribution of charge carriers will lead to a modification of exchange interactions and the appearance of complex magnetic structures. Many results of magnetic measurements indicate the existence of an antiferromagnetic (AFM) phase of a G type in $R_xCa_{1-x}MnO_3$ crystals with $x < 0.05$ [5] and the existence of another G phase with a canted structure, as well as of phases of the C type in the range of intermediate concentrations $0.05 < x < 0.2$ in compounds doped with Pr, Nd, and Sm. The coexistence of phases was revealed in $La_xCa_{1-x}MnO_3$ [6] with $x = 0.1$ and 0.12 by neutron diffraction. The nonstoichiometry with respect to oxygen substantially widens the region of coexistence. Thus, the range of coexistence of phases such as AFM insulator of the C type and an AFM insulator of the G type with a canted structure becomes expanded to $0.05 < x < 0.12$ due to a deficit in oxygen, which is a source of charge carriers (electrons) [7]. Vacancies in oxygen lead to stronger Mn–O distortions, unlike the case of substitution of La for Ca. In $CaMnO_{3-\delta}$, ordering of oxygen vacancies has been revealed [8].

This paper is aimed at the determination of conditions under which phase separation is developed and a canted magnetic structure arises. In the region of large concentrations, the perovskite-like structure in manganites exists only in Ca-containing compounds; in the case where A = Sr, Ba, and Pb, there arises a hexagonal structure [9]. The replacement of calcium ions by rare-earth elements in $CaMnO_3$ leads to common regularities: there arises a sequence of magnetic structures of the G type (an antiferromagnetic structure of the Néel type) and C type (spins have a ferromagnetic ordering in one direction of the cubic structure and an antiferromagnetic ordering in the plane orthogonal to this direction).

2. MODEL

A nonstoichiometric substitution of rare-earth ions for calcium leads to local changes in the potential of the electric field and produces excess electrons, which are

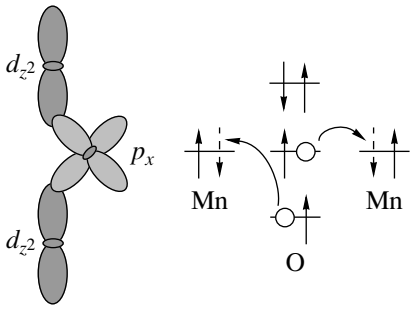

Fig. 1. Model of virtual exchange of electrons at various oxygen orbitals.

located at e_g levels of manganese ions. These electrons are hybridized with electrons located at the p orbitals of oxygen. The energy of hybridization of electrons calculated using two-center integrals ($pd\sigma$) and ($pd\pi$) at p_z and $d_{3z^2-r^2}$ orbitals exceeds the energy of hybridization at p_x and $d_{x^2-y^2}$ orbitals by almost 20% and is equal to $E_{z,3z^2-r^2}/E_{x,x^2-y^2} = 2/\sqrt{3}$ [10]. The local distortions of the structure caused by rare-earth elements induce additional virtual transitions and hybridization of $p_{x,y}$ and $d_{3z^2-r^2}$ orbitals. As a result, there becomes possible a transition of electrons between neighboring manganese ions through an oxygen ion with an exchange of an electron between oxygen p_z and $p_{x,y}$ orbitals.

Strong Hund exchange between p electrons retains spin polarization upon the virtual Mn–Mn transition. The matrix element of hopping $t(\mathrm{Mn}_i\mathrm{Mn}_{i+1}) = (V_{z,3z^2-r^2}V_{x,y,3z^2-r^2})/(e_p - e_d + U_d - U_p)$, where $e_p - e_d$ is the energy of the gap for the transfer of charge from Mn to O, is equal to 3 eV [11]; U_d and U_p are the corresponding parameters of the Coulomb interaction ($U_d - U_p$ = 2–4 eV) [11]; and $V_{z,3z^2-r^2}$ and $V_{x,y,3z^2-r^2}$ are the integrals of overlap between the electron orbitals. The parameter $V_{z,3z^2-r^2}$ is well known for manganites (≈2 eV); the magnitude of $V_{x,y,3z^2-r^2}$ can only be estimated qualitatively. Thus, with decreasing Mn–O–Mn valence angle θ (for an ideal cubic structure, this angle is θ = π), this parameter will increase as $V_{x,y,3z^2-r^2} \sim \langle\sin\theta\rangle$. The magnitude of this angle was determined for a number of elements; thus, $|\cos\theta| = 0.91$ for La, 0.88 for Pr, 0.86 for Nd, and 0.84 for Sm [12]; correspondingly, the magnitude of the ferromagnetic exchange interaction increases.

This model explains an increase in the Néel temperature of an antiferromagnet with increasing ferromagnetic ordering of spins in a chain; thus, T_N = 120 K for $Ca_{1-x}La_xMnO_3$ [13], 235 K for $Ca_{1-x}Pr_xMnO_3$, and 250 K for $Ca_{1-x}Sm_xMnO_3$ [5] at $x = 0.3$.

3. MAGNETIC ORDERING

In our model, formation of a ferromagnetic interaction induced by virtual exchange of electrons at various orbitals of oxygen is possible in the vicinity of a rare-earth element (Fig. 1). The splitting of p orbitals of an apical oxygen is also caused by the change in the local symmetry of crystal structure. Thus, beginning already with a concentration $x = 0.06$, there is observed a nucleation of a monoclinic crystal structure. In the monoclinic C-type AFM phase, orbital ordering is realized [14], which can be represented in the form of equivalent spin operators of creation and annihilation of the orbital moment. Orbital ordering can substantially change the magnitude and even the sign of exchange interaction. The effective Hamiltonian obtained from the many-electron Hamiltonian [15] can be represented through spin operators as

$$H = -\sum_{ij\alpha} J_{i,j} S_i^\alpha S_j^\alpha - \sum_{ij\alpha} A_{i,j}^{\alpha\alpha} \tau_i^\alpha \tau_j^\alpha - 4\sum_{ilm\alpha} K_{i,j,l,m} S_i^\alpha S_j^\alpha \tau_l^\sigma \tau_m^\alpha, \quad (1)$$

where J_{ij} is the exchange interaction, A is the parameter of the orbital interaction, and K_{ijlm} is the parameter of the interrelation between the orbital and spin subsystems. In reality, the Hamiltonian is strongly anisotropic in pseudospins τ, and the effective exchange $J_{ij}^{\mathrm{eff}} = J_{ij} + 4K_{ijlm}\langle\tau_l^\alpha\tau_m^\alpha\rangle$ between the pair of spins of manganese ions along the OZ axis also will be anisotropic.

The magnetic structure of calcium manganite doped with rare-earth elements can be calculated using a Hamiltonian with random anisotropic bonds. The substitution of ions of a rare-earth element for calcium ions leads to a change of the sign of exchange interaction and induces anisotropy of exchange between two nearest Mn–Mn bonds. The Hamiltonian has the form

$$H = -\sum_{ij} (J_{i,j}^{zz} S_i^z S_j^z + J_{ij}^p (S_i^x S_j^x + S_i^y S_j^y)), \quad (2)$$

where the parameters of exchange are randomly distributed over the lattice in the direction [001]:

$$P(J_{i,i+z}^{zz}) = (1-x)\delta(J_{i,i+z}^{zz} - J) + x\delta(J_{i,i+z}^{zz} - A);$$
$$P(J_{i,i+z}^{p}) = (1-x)\delta(J_{i,i+z}^{p} - J) + x\delta(J_{i,i+z}^{p} - K), \quad (3)$$

where $J < 0$, $A > 0$, and $K > 0$ are the antiferromagnetic, ferromagnetic, and exchange interactions between nearest neighbors; A and K are randomly distributed along the OZ axis; and S is the classical spin with components S (cosθ, sinθcosφ, sinθsinφ). To calculate magnetic characteristics, the Monte Carlo method is used with periodic boundary conditions on a lattice with dimensions $N = 18 \times 18 \times 18$ and the number of steps of 5000–10000 MC/spin. The magnetic structure was determined from the spin–spin correlation function cal-

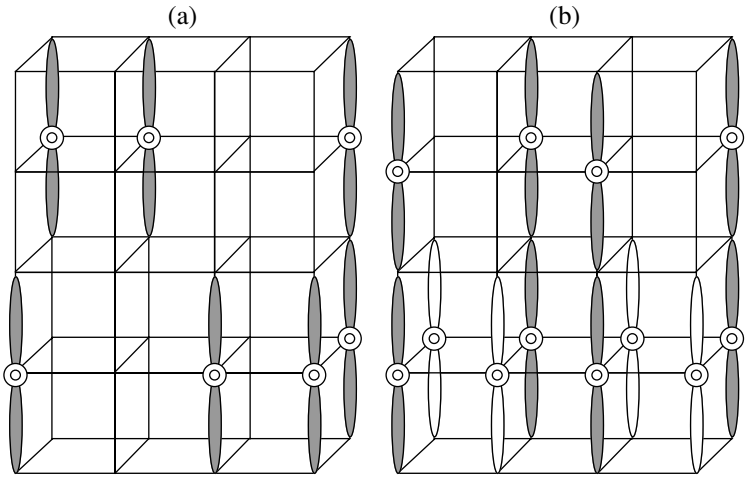

Fig. 2. Model with (a) a random and (b) ordered arrangement of bonds over the lattice.

culated along the longitudinal and transverse components of spin along the three edges of the computational cube.

Apart from a random distribution of bonds, a certain order in the disposition of ferromagnetic bonds was specified, which imitated phase separation. The physical factor that leads to phase separation is a substantial loss in exchange energy as compared to the energy of electrostatic interaction. Thus, the substitution of FM bonds for the AFM ones occurs first on one of the sublattices, whose sites are located along the diagonals of the squares, as is shown in Fig. 2b. The length of a chain with substituted FM bonds increases with increasing concentration; after the complete substitution, the next sublattice starts to be filled.

Figure 3 displays dependences of spin–spin correlation functions between the longitudinal and transverse spin components at a random and ordered arrangement of bonds. In the intermediate region of concentrations $x_1 < x < x_2$, there exists a long-range magnetic order between the longitudinal and transverse spin components. Such a state is characteristic of a canted antiferromagnet. In the case of an ordered arrangement of bonds, the region of existence of a canted AFM becomes strongly narrowed ($x_1 \approx 0.1, x_2 \approx 0.16$) as compared to the random distribution of bonds, in which case the region of coexistence of *G*-type and *C*-type phases depends on the exchange parameters and varies from $0.1 < x < 0.15$ to $0.1 < x < 0.25$. The magnetic structure of a canted AFM can be represented as a *G*-type structure with respect to longitudinal spin components and a *C*-type structure for transverse components. A decrease in the exchange energy by the absolute value at a random substitution of bonds in a concentration range of $x_1 < x < x_2$ is $\Delta E = (E_{\text{random}} - E_{\text{ordering}}) \sim KS^2$ and virtually vanishes above the Néel temperature (Fig. 4a). The concentration dependences of the energy of a stochastic AFM with two types of bond distribution are given in Fig. 4b.

The Néel temperatures were determined from spin–spin correlation functions calculated along various directions in the cube. Figure 5 displays typical temperature dependences of spin–spin correlation functions at a distance $r/a = 5$ for longitudinal (Fig. 5a) and transverse spin components (Figs. 5b, 5c) at various relationships between the exchange parameters at an ordered arrangement of bonds. The critical concentration at which the correlator $\langle S_i^x S_{i+5}^x \rangle_{[001]} > 0$ along the *OZ* axis has a negative value in the plane $\langle S_i^x S_{i+5}^x \rangle_{(001)} < 0$

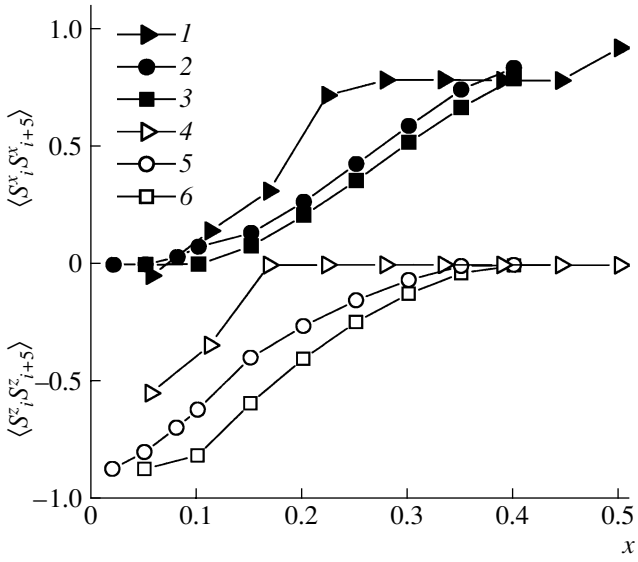

Fig. 3. Spin–spin correlation functions $\langle S_i^\alpha S_{i+5}^\alpha \rangle$ of longitudinal ($\alpha = x$) and transverse ($\alpha = z$) components depending on concentration for (*1*, *4*) an ordered arrangement of bonds at $K/J = 4$ and $A/J = 0.03$, (*2*, *5*) random arrangement at $K/J = 4$, $A/J = 0.03$, and (*3*, *6*) random arrangement at $K/J = 2$ and $A/J = 0.06$.

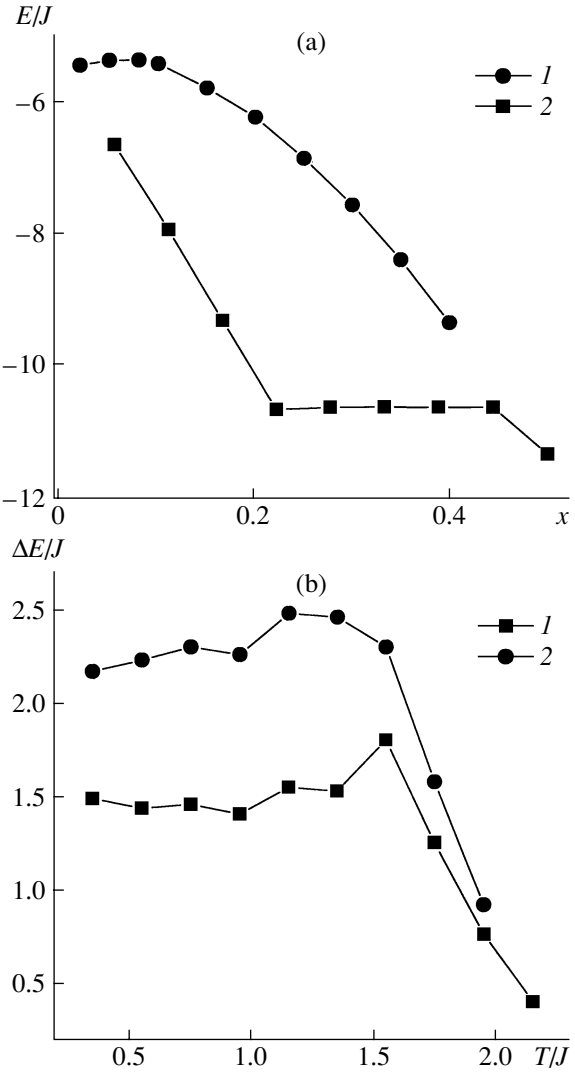

Fig. 4. (a) The concentration dependence of the energy E/J of an AFM with (*1*) a random and (*2*) an ordered arrangement of bonds on the lattice with exchange parameters $K/J = 4$ and $A/J = 0.03$ on concentration; and (b) the temperature dependence of the energy difference $\Delta E = (E_{\text{random}} - E_{\text{ordering}})$ of AFMs with a random and ordered arrangement of bonds on the lattice with exchange parameters $K/J = 2$ and $A/J = 0.5$ at concentrations (*1*) $x = 0.05$ and (*2*) 0.2.

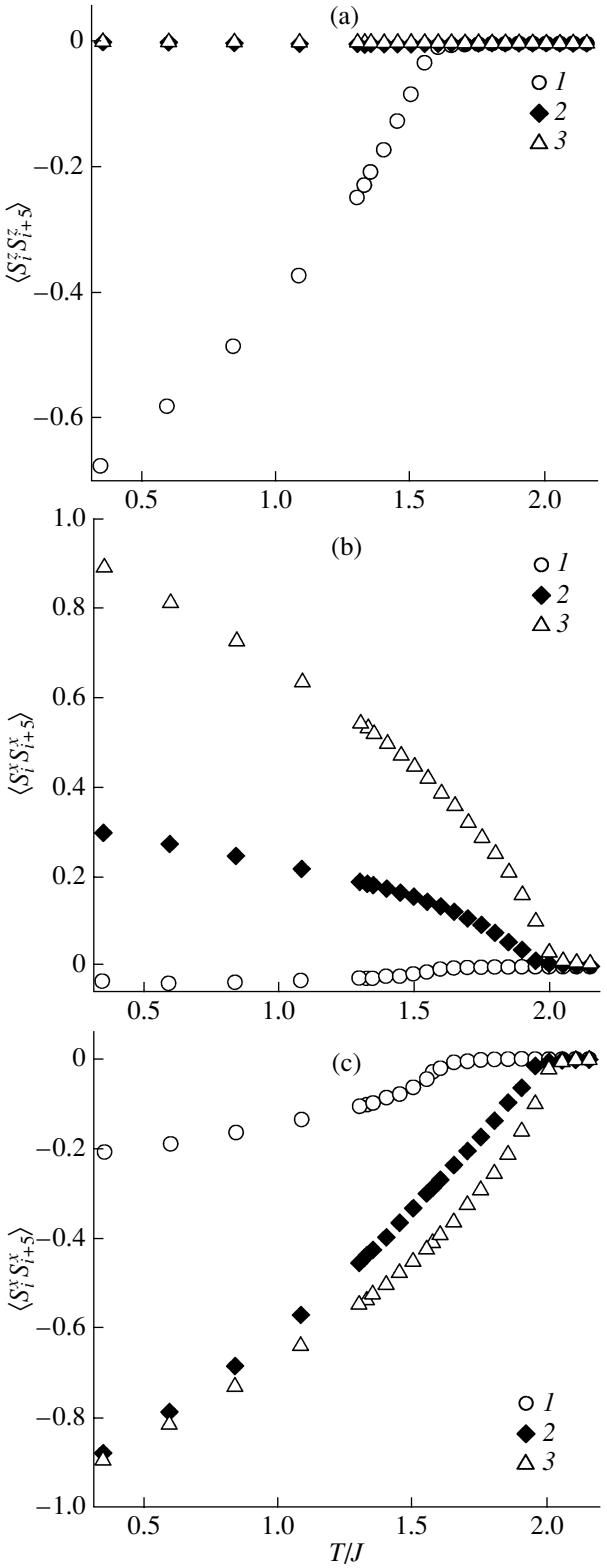

Fig. 5. Temperature dependences of spin–spin correlation functions $\langle S_i^\alpha S_{i+5}^\alpha \rangle$ of (a) longitudinal ($\alpha = zz$) and (b, c) transverse ($\alpha = x, y$) spin components in AFMs with an ordered arrangement of bonds at a distance $r/a = 5$ along (a, b) [001] direction and (c) in the plane (001) for $K/J = 2$ and $A/J = 0.06$ at concentrations (a) $x = 0.03$, (b) 0.165, and (c) 0.48.

is associated with a changeover from the *G*-type to *C*-type magnetic order.

Figure 6 displays normalized dependences of the Néel temperature on concentration. The isotropic FM bond does not lead to the formation of a *C*-type phase, and the antiferromagnetic state is destroyed at the critical concentration x_c with the formation of a spin glass (the AFM-phase field is shown by a dashed line in Fig. 6a). A comparison with experimental data permits us to select a proper model of distribution of bonds over the lattice. Thus, for $Ca_{1-x}La_xMnO_3$ the best agreement with experimental data [13] is achieved at a random distribution of bonds with the parameters $A/J = 0.5$ and

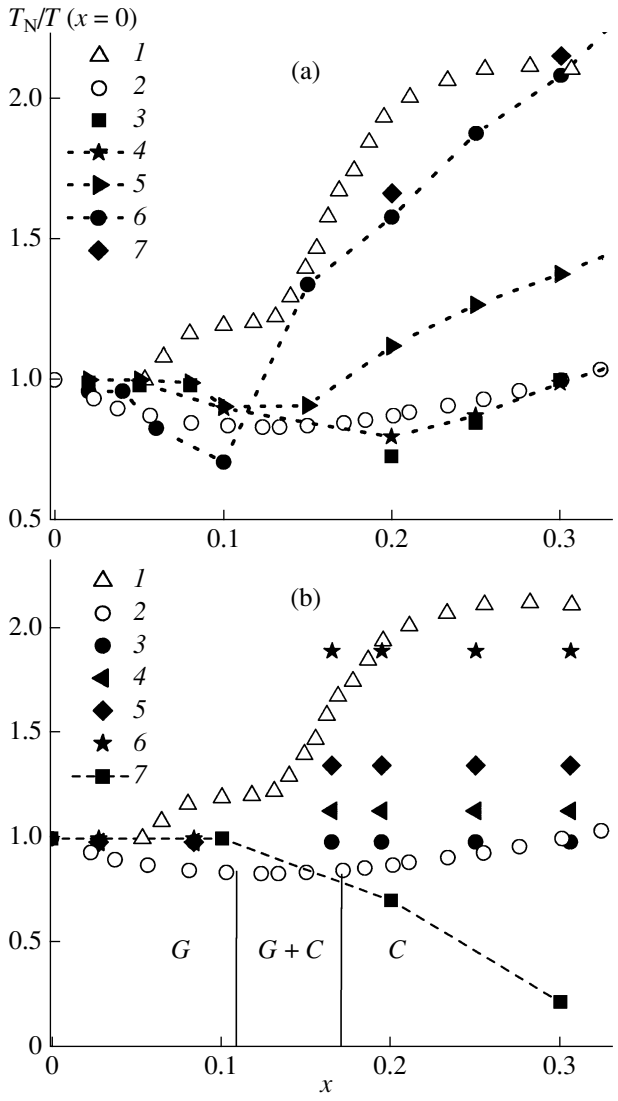

Fig. 6. Concentration dependences of the normalized Néel temperature $T_N(x)/T_N$ ($x = 0$): (*1*, *2*) experimental data [3] and (*3*–*7*) theoretical results at (a) a random and (b) layered arrangement. (a) (*3*) $K/J = 2$, $A/J = 0.06$; (*4*) $K/J = 2$, $A/J = 0.5$; (*5*) $K/J = 4$, $A/J = 0.03$; (*6*) $K/J = 10$, $A/J = 0.03$; (*7*) $K/J = 10$, and $A/J = 0.5$. (b) (*3*) $K/J = 1$, $A/J = 0.03$; (*4*) $K/J = 1.5$, $A/J = 0.03$; (*5*) $K/J = 2$, $A/J = 0.06$; (*6*) $K/J = 4$; $A/J = 0.03$; and *7*) $A = K$, $K/J = 1.7$. Lines indicate the regions of coexistence of antiferromagnetic *G*-type and *C*-type phases.

$K/J = 2$; for $Ca_{1-x}Pr_xMnO_3$, the experimental data on the temperature dependence $T_N(x)/T_N(x = 0)$ is satisfactorily described by a model with an ordered arrangement of bonds with $A/J = 0.03$ and $K/J = 4$.

4. CONCLUSIONS

Virtual exchange by electrons between the $d_{3z^2-r^2}$ orbitals through various $p_{z,x,y}$ orbitals of oxygen can induce anisotropic ferromagnetic exchange. The model in which a substituting lanthanum ion randomly induces an anisotropic ferromagnetic bond explains the changeover from the *G*-type to *C*-type magnetic order with the formation of a canted antiferromagnet in the region of the concentration transition. The substitution of Pr and Sm ions for Ca ions leads to ordering of anisotropic ferromagnetic bonds and, possibly, is one of the mechanisms of the observed phase separation in these compounds. Parameters of exchange interactions at which the calculated concentration dependences of the Néel temperature satisfactorily agree between themselves have been found.

ACKNOWLEDGMENTS

This work was supported by the State Program no. 02.513.11.31.08.

REFERENCES

1. E. L. Nagaev, "Lanthanum Manganites and other Giant-Magnetoresistance Magnetic Conductors," Usp. Fiz. Nauk **166** (8), 833–858 (1996) [Phys.–Usp. **39** (8), 781–805 (1996)].
2. L. P. Gor'kov, "Lattice and Magnetic Effects in Doped Manganites," Usp. Fiz. Nauk **168** (6), 665–671 (1998) [Phys.–Usp. **41** (6), 589–594 (1998)]; M. Yu. Kagan and K. L. Kugel' "Inhomogeneous Charge Distributions and Phase Separation in Manganites," Usp. Fiz. Nauk **171** (6), 577–596 (2001) [Phys.–Usp. **44** (6), 553–570 (2001)].
3. Yu. A. Izyumov and Yu. N. Skryabin, "Double Exchange Model and the Unique Properties of the Manganites," Usp. Fiz. Nauk **171** (2), 121–148 (2001) [Phys.–Usp. **44** (2), 109–134 (2001)].
4. H. Chiba, M. Kikuchi, and K. Kusaba, "Ferromagnetism and Large Negative Magnetoresistance in $Bi_{1-x}Ca_xMnO_3$ ($x \geq 0.8$) Perovskite," Solid State Commun. **99** (7), 499–502 (1996).
5. C. Martin, A. Maignan, M. Hervieu, and B. Raveau "Magnetic Phase Diagrams of $L_{1-x}A_xMnO_3$ Manganites (L = Pr, Sm; A = Ca, Sr)," Phys. Rev. B: Condens. Matter Mater. Phys. **60** (17), 12191–12199 (1999).
6. C. D. Ling, E. Granado, J. J. Neumeier, et al., "Inhomogeneous Magnetism in La-Doped $CaMnO_3$. I. Mesoscopic Phase Separation Due to Lattice-Coupled Ferromagnetic Interactions," Phys. Rev. B: Condens. Matter Mater. Phys. **68**, 134439 (2003).
7. N. N. Loshkareva, A. V. Korolev, N. I. Solin, et al., "Magnetic, Electrical, and Optical Properties of Electron-Doped —$Ca_{1-x}La_xMnO_{3-\delta}$ ($x \leq 0.12$) Single Crystals," Zh. Eksp. Teor. Fiz., **129** (2), 283–293 (2006) [J. Exp. Theor. Phys. **102** (2), 248–257 (2006)].
8. S. F. Dubinin, N. N. Loshkareva, S. G. Teploukhov, et al., "Ordering of Oxygen Vacancies in a $CaMnO_{3-\delta}$ Perovskite Single Crystal," Fiz. Tverd. Tela (S.-Peterburg) **47** (7), 1226–1231 (2005) [Phys. Solid State **47** (7), 1267–1272 (2005)].
9. W. C. Koehler, Jr., E. F. Bertaut, H. L. Yakel, and E. F. Forrat, "On the Crystal Structure of the Manga-

nese(III) Trioxides of the Heavy Lanthanides and Yttrium," Acta Crystallogr. **16**, 957–962 (1963).

10. P. Mahadevan, N. Shanthi, D. D. Sarma, "Estimates of Electronic Interaction Parameters for LaMO$_3$ Compounds (M = Ti–Ni) from *ab initio* Approaches," Phys. Rev. B: Condens. Matter Mater. Phys. **54** (16), 11199–11206 (1996).
11. J. C. Slater and G. F. Koster, "Simplified LCAO Method for the Periodic Potential Problem," Phys. Rev. **94** (6), 1498–1524 (1954).
12. J.-S. Zhou and J. B. Goodenough, "Orbital Order–Disorder Transition in Single-Valent Manganites," Phys. Rev. B: Condens. Matter Mater. Phys. **68**, 144406 (2003).
13. M. Pissas and G. Kallias, "Phase Diagram of the $La_{1-x}Ca_xMnO_3$ Compound $0.5 \le x \le 0.9$)," Phys. Rev. B: Condens. Matter Mater. Phys. **68**, 134414 (2003).
14. E. Granado, C. D. Ling, J. J. Neumeier, et al., "Inhomogeneous Magnetism in La-Doped $CaMnO_3$. II. Nanometric-Scale Spin Clusters and Long-Range Spin Canting," Phys. Rev. B: Condens. Matter Mater. Phys. **68**, 134440 (2003).
15. K. I. Kugel' and D. I. Khomskii, "Jahn–Teller Effect and Magnetism: Transition-Metal Compounds," Usp. Fiz. Nauk **136** (4), 621–664 (1982).